

Supplement of Atmos. Chem. Phys., 19, 5511–5528, 2019
<https://doi.org/10.5194/acp-19-5511-2019-supplement>
© Author(s) 2019. This work is distributed under
the Creative Commons Attribution 4.0 License.



Supplement of

Large-scale transport into the Arctic: the roles of the midlatitude jet and the Hadley Cell

Huang Yang et al.

Correspondence to: Huang Yang (hyang61@jhu.edu)

The copyright of individual parts of the supplement might differ from the CC BY 4.0 License.

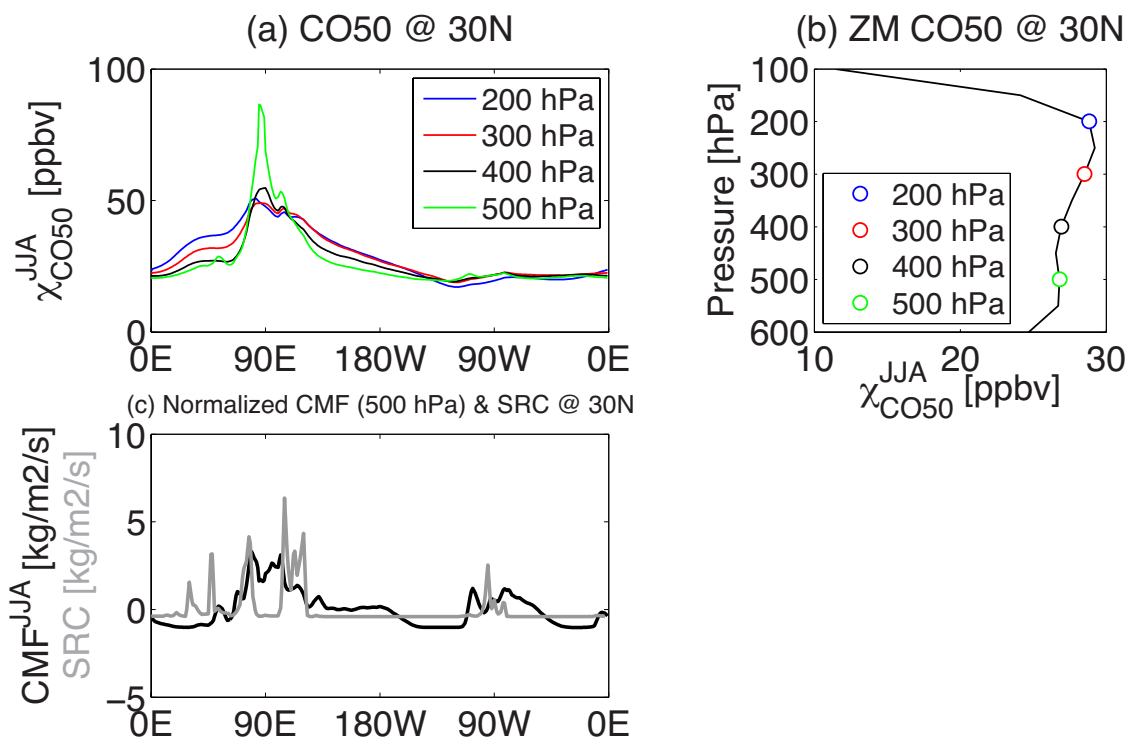


Figure S1. Relations among emission, convection, and CO50 concentration during JJA: (a) longitudinal distribution of CO50 at 30°N for various vertical levels from 200 hPa to 500 hPa; (b) vertical profile of zonal-mean CO50 concentration at 30°N highlighting the values at a few vertical levels that are shown in (a); and (c) 500 hPa CMF (black) and surface CO50 emissions (gray) at 30°N.

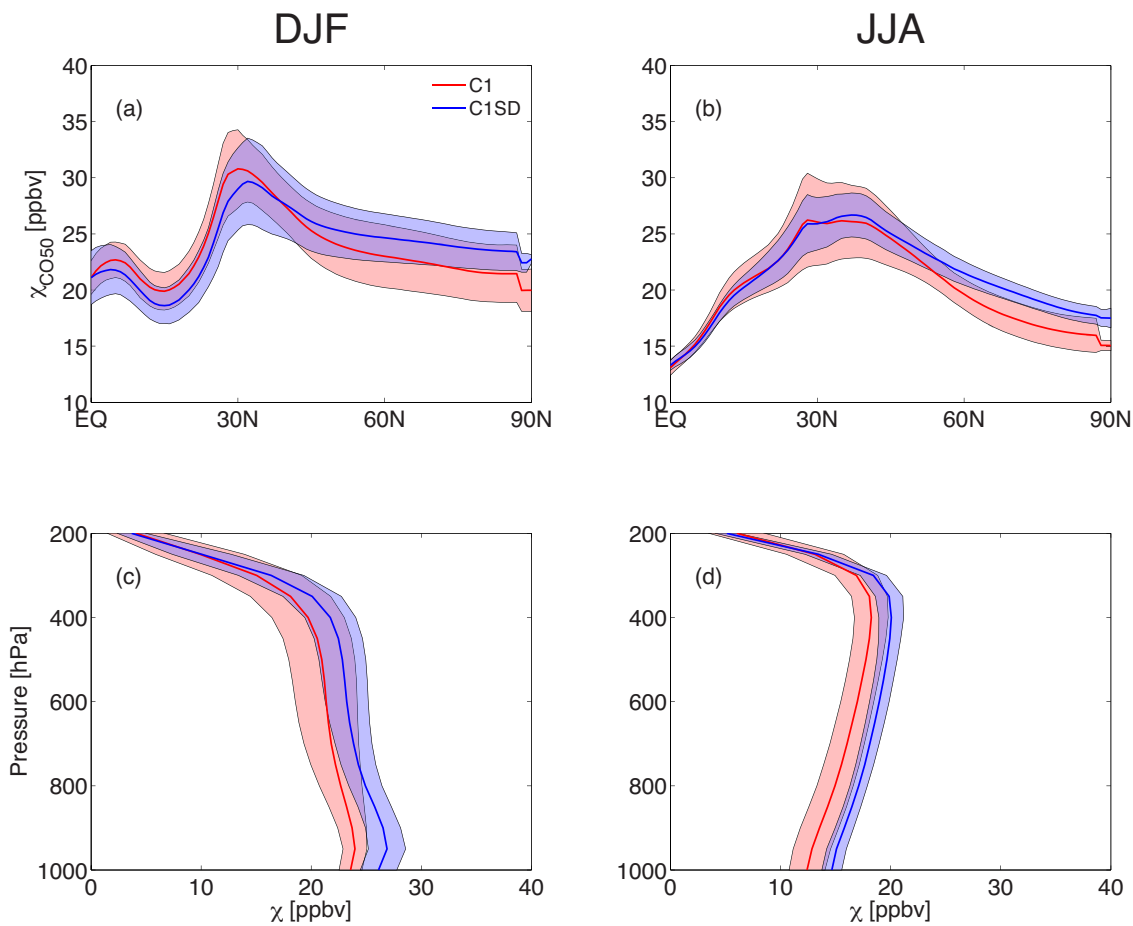


Figure S2. Similar to Fig.2, but showing the multi-model mean of CO50 concentrations in C1 and C1SD simulations (red and blue lines respectively), as well as the multi-model spread (denoted by one-standard deviation as shades).

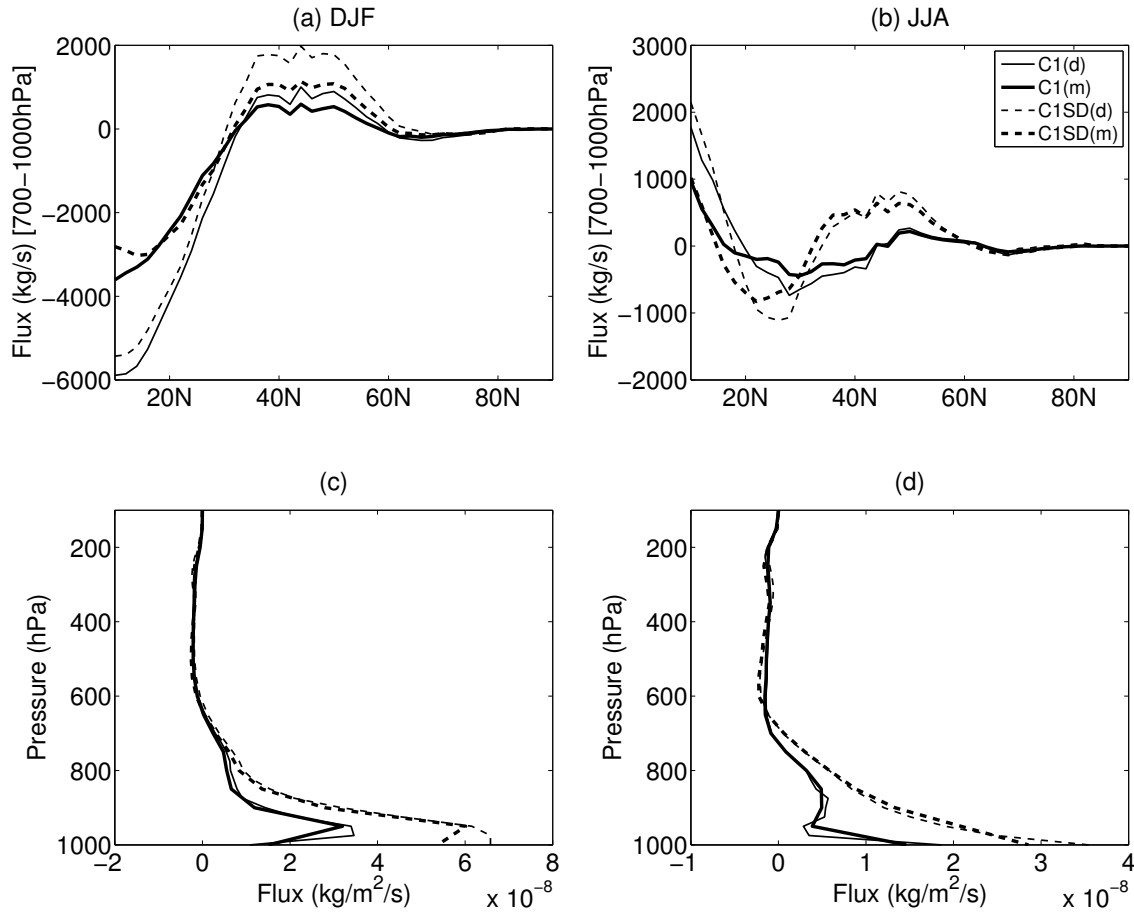


Figure S3. (a,b) Similar to Fig.8, but comparing zonal-mean fluxes in two GEOS simulations (i.e., GEOS-C1 and GEOS-C1SD) derived from daily output (light lines) with ones derived from interpolated monthly output (bold lines) in GEOS-C1 (solid) and GEOS-C1SD (dashed). (c,d) Similar to (a,b), but showing vertical profile of tracer mass flux (units: $\text{kg m}^{-2} \text{s}^{-1}$) at 50°N .

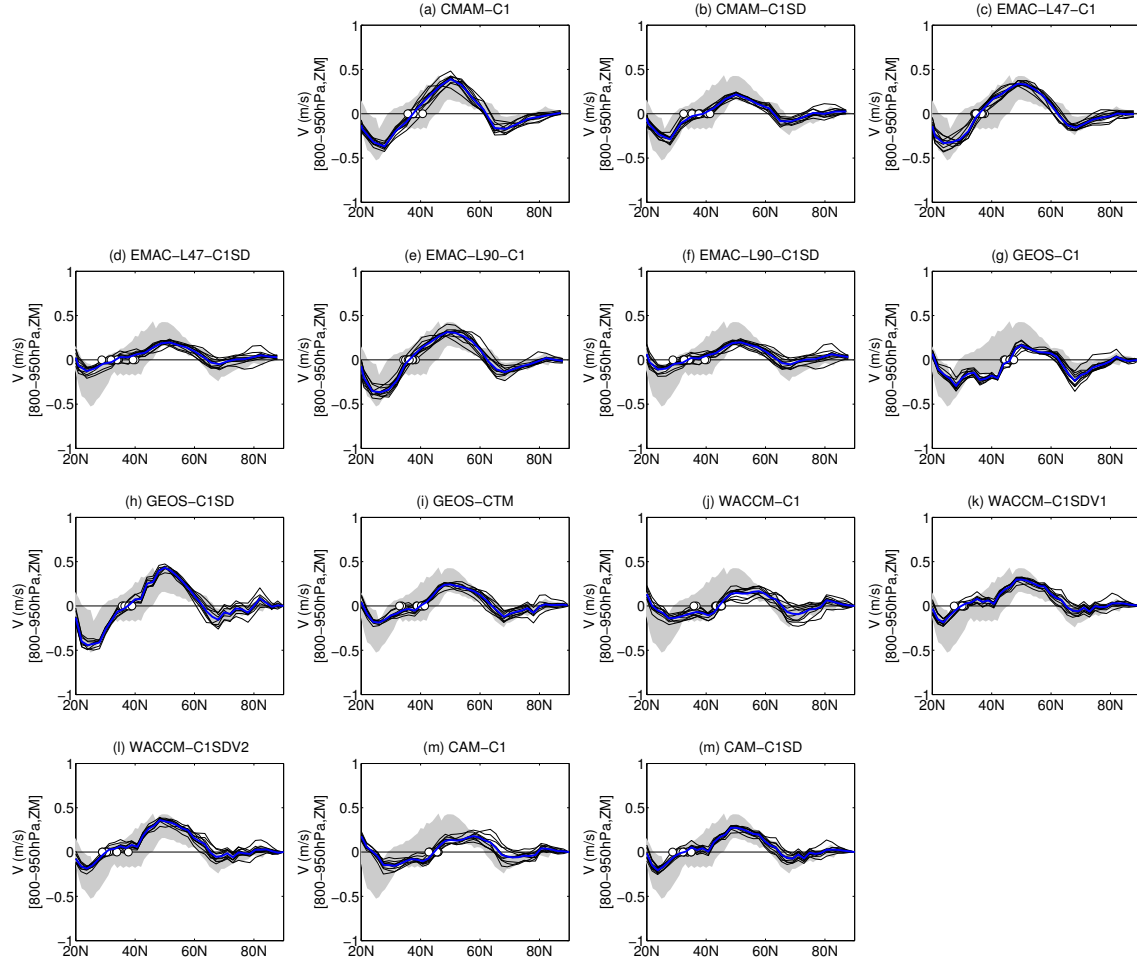


Figure S4. Latitudinal profile of JJA low-level zonal-mean meridional wind \bar{v} (800 – 950 hPa) in each simulation. The black lines and circles denote the interannual variations of \bar{v} and $\phi_{v=0}$ within the model, while gray shades give the multi-model spread among model climatology, as shown in Figure 10(a). The blue thick line denotes the climatological v of the simulation.

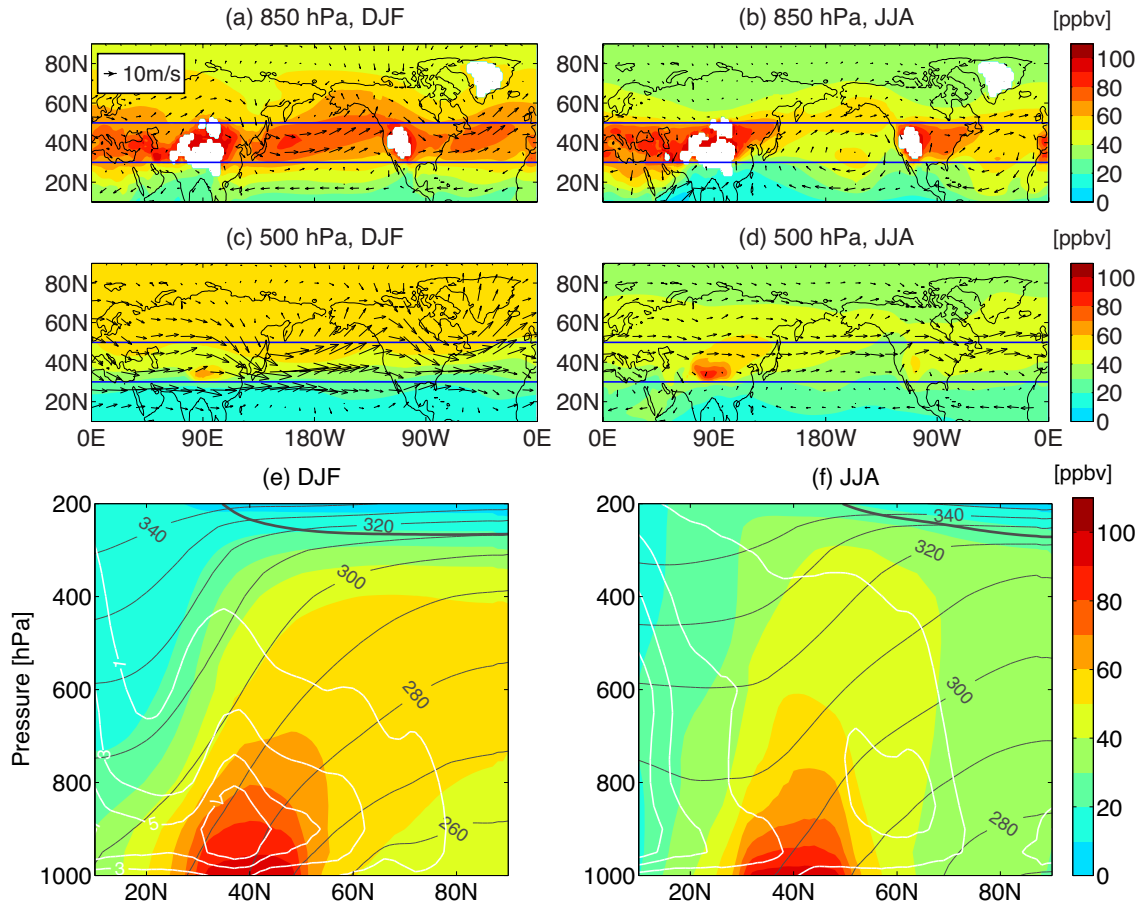


Figure S5. Similar to Fig.1, but for NH50.

Table S1. Correlation coefficients between Arctic CO50 concentration and physical process related metrics (such as convective mass flux (CMF), ϕ_{jet} , mean flux, and $\phi_{v=0}$ as listed in the 1st column, definitions of metrics followed the same fashion as in the manuscript) calculated using all available models versus only the free-running (C1) models versus clustered models (i.e., exclude NIWA-C1 for similarity to ACCESS-C1, exclude EMAC-L90-C1/C1SD for similarity to EMAC-L47-C1/C1SD, exclude WACCM-C1SDV2 for similarity to WACCM-C1SDV1, and exclude CAM-C1/C1SD for similarity to WACCM-C1/C1SDV1). Calculation of correlation is based on climatology, and those are statistically significant (95%) are marked in **bold**.

	DJF			JJA		
	All	C1	Cluster	All	C1	Cluster
CMF	0.05	-0.10	0.19	0.05	0.29	0.15
ϕ_{jet}	-0.63	-0.92	-0.64	-0.84	-0.79	-0.83
mean flux	0.69	0.68	0.69	0.78	0.96	0.79
$\phi_{v=0}$	-0.76	-0.95	-0.76	-0.58	-0.70	-0.51

Table S2. Correlation coefficients between mean meridional flux over high latitudes (60°N-80°N) and Arctic CO50 concentrations (500-800 hPa, 70°N-90°N, zonal mean). For mean meridional flux over high latitudes, it is vertically integrated in the low levels (700-1000 hPa) during DJF but in the upper levels (300-500 hPa) during JJA, considering differences in the CO50 vertical maximum between seasons (Fig. 1(e,f) and Fig. 2(c,d)). The correlation between climatologies among models are shown in the 2nd row (similar to results shown in Fig. 9 (b,d)), while interannual correlations in individual simulations are shown in the rows below. Coefficients that are statistically significant (95%) are marked in **bold**.

Models	DJF	JJA
Climatology among models	0.28	0.37
CMAM-C1	0.67	-0.26
CMAM-C1SD	0.35	0.74
EMAC-L47-C1	0.50	0.22
EMAC-L47-C1SD	0.43	0.60
EMAC-L90-C1	0.51	-0.25
EMAC-L90-C1SD	0.43	0.55
GEOS-C1	0.88	0.70
GEOS-C1SD	0.12	0.75
GEOS-CTM	0.46	0.84
WACCM-C1	-0.02	0.52
WACCM-C1SDV1	0.09	0.78
WACCM-C1SDV2	0.53	0.83
CAM-C1	0.50	0.51
CAM-C1SD	0.15	0.75